Understanding the role of respresentation in controlled quantum-dynamical mechanism analysis

Abhra Mitra[*]

Department of Electrical Engineering, Princeton University, Princeton, New Jersey 08544, USA

Ignacio R. Sola

Departamento de Quimica Fisica I, Universidad Complutense, 28040 Madrid, Spain

Herschel Rabitz

Department of Chemistry, Princeton University, Princeton, New Jersey 08544, USA

Hamiltonian Encoding (HE) has been proposed as a technique for analyzing the mechanism of controlled quantum dynamics, where mechanism is understood in terms of the set of amplitudes of the dominant pathways connecting the initial and final states of the system. The choice of representation for the system wave function is often motivated by seeking simplicity for the structure of the Hamiltonian and not necessarily for the generated dynamics. However, the mechanism revealed by HE is strongly dependent on the basis in which the wave function is represented. The degree of mechanistic complexity is indicated by the relevant orders of the Dyson series contributing to the dynamics. An appropriate choice of representation can yield a simpler view of the dynamical mechanism by shifting some of the complexity into the representation itself. In this work the choice of representation is set up as the solution to a variational optimization problem. For unconstrained basis transformations, the optimization of the representation is formally equivalent to solving the time-dependent Schrödinger equation; different constrained basis transformations provide distinct dynamical perspectives. Specific constrained variational *Ansätze* are compared and analyzed by performing HE on several simple Hamiltonians with an observation of the extent to which the mechanism assessment varies with representation. The general variational formulation for determining representation can flexibly admit other *Ansätze* with the ultimate aim of balancing the ease of determining and understanding the representation with the reduction in mechanistic complexity.

I. INTRODUCTION

The control of quantum dynamics has many potential applications in science and engineering, and a number of techniques have been proposed to achieve quantum control. Optimal control theory (OCT) [1–4], provides a general framework for this purpose and closed-loop techniques using OCT are meeting with broad success in the laboratory [5–12]. The resultant controlled dynamics can be complex in keeping with the nature of the system and the objectives. The control mechanisms have often remained obscure, as the experiments are directed at achieving control and not towards an assessment of the mechanism. The Hamiltonian encoding (HE) procedure was proposed [13] as a method for organizing and understanding the dynamics created by complex control fields. HE has been used for mechanism assessment of various problems [13–16] in the context of computer simulations. This paper studies systems that can be represented by a d-dimensional Hilbert space, where the dynamics is governed by the propagator $U(t)$, satisfying the time-dependent Schrödinger equation (TDSE)

$$i\frac{dU(t)}{dt} = H(t)U(t), \tag{1}$$

where $\hbar$ is included in the Hamiltonian H. HE organizes the information in Eq. (1) in terms of the Dyson series for the time evolution operator

$$U(t) = I + (-i)\int_0^t H(t_1)dt_1 + (-i)^2 \int_0^t H(t_2)\int_0^{t_2} H(t_1)dt_1 dt_2$$

$$+ \cdots . \tag{2}$$

It can be shown [13] that this expansion will always converge for systems of finite dimension, evolving over a finite period of time $[0,T]$ under a bounded control field. HE utilizes this expansion to introduce the concept of control pathways. Section II will give further details defining the pathways. With HE the control mechanism is expressed in terms of the significantly contributing control pathways, which are specified by the integrals in Eq. (2). For simulations, the integrals in the series expansion are computationally difficult to evaluate, especially for high intensity fields, where the series typically converges only after many terms. Computationally, HE evaluates the integrals in Eq. (2) by introducing a timelike variable s and creating a family of Hamiltonians $H(t,s)$ parametrized by s. These parametrized Hamiltonians have a specific encoded relation to the original Hamiltonian $H(t)$, including the criterion $H(t)=H(t,s=0)$. By evaluating $U(T,s)$ over these Hamiltonians as a function of s, it is possible to determine the dynamical pathways in the original system $U(T)\equiv U(T,s=0)$ at a chosen time T.

*abhra@princeton.edu

On the other hand, a quantum-mechanical system may be represented over a set of basis states, and the choice of this basis is flexible, often dictated by convention or convenience. The nature of the mechanism deduced by HE is, however, dependent on this choice of representation. A previous work [14] studied the impact of a change of representation on mechanism in the context of systems controlled using the STIRAP procedure [17], in which a counterintuitive sequence of two pulses (the Stokes pulse preceding the pump pulse) drives the population in a three-level system. This system had two "natural" choices of representation: either the eigenstates of the field-free Hamiltonian H_0, or the dressed states of the system coupled with the field. As the control field intensity was ramped up, and the population transfer became more adiabatic, the mechanism in the H_0 representation became increasingly more complex, while in the dressed states representation it became increasingly simpler. This illustration highlighted the important role played by the choice of representation in the mechanism analysis.

This work studies the impact of the choice of representation on mechanism in a more general manner. The remainder of this paper is organized as follows. Section II presents a brief review of the HE concept [13]. Section III sets up the choice of representation as an optimization problem, and presents a simple formulation and its solution. Section IV generalizes the optimization procedure of Sec. III to cover a larger class of representation changes. Section V illustrates the effect of an optimal change of representation with some numerical examples. Finally, the results are summarized along with conclusions in Sec. VI.

II. THE HAMILTONIAN ENCODING TECHNIQUE

As the developments in this paper build on the original HE procedure [13], a brief summary is presented in this section. Consider the evolution of a quantum system where the dynamics evolve in a d-dimensional state space, whose time evolution is given by Eq. (1). The goal of HE is to understand the mechanism by which $H(t)$ transfers amplitude from some initial state $|a\rangle$ to the final state $|b\rangle$; therefore, we consider the relevant matrix element $U_{ba}(T)$. Rewriting Eq. (2) to focus on U_{ba}, produces

$$U_{ba}(T) = \langle b|a\rangle + \int_0^T \langle b|H(t_1)|a\rangle dt_1$$

$$+ \sum_{l=1}^d \int_0^T \int_0^{t_2} \langle b|H(t_2)|l\rangle\langle l|H(t_1)|a\rangle dt_1 dt_2 + \cdots .$$

$$(3)$$

To simplify the equations we define $h_{lm} = \langle l|H(t)|m\rangle$ and introduce the notation [13]

$$U_{ba}^{n(l_1,l_2,\ldots,l_{n-1})} = \int_0^T \int_0^{t_n} \cdots \int_0^{t_2} h_{bl_{n-1}}(t_n) h_{l_{n-1}l_{n-2}}(t_{n-1}) \cdots$$

$$\times h_{l_1a}(t_1) dt_1 \cdots dt_{n-1} dt_n,$$

$$(4)$$

so that Eq. (3) becomes

$$U_{ba} = \sum_{n=0}^\infty \sum_{l_1,l_2,\ldots,l_{n-1}=1}^d U_{ba}^{n(l_1,l_2,\ldots,l_{n-1})}.$$

$$(5)$$

A quantum pathway is defined as a sequence of transitions starting from $|a\rangle$ and ending at $|b\rangle$. Each pathway corresponds to one of the individual integrals in the expansion of $U_{ba}(T)$, with the amplitude of the pathway $(a \rightarrow l_1 \cdots \rightarrow l_{n-1} \rightarrow b)$ being $U_{ba}^{n(l_1,l_2,\ldots,l_{n-1})}$. The order of a pathway n is the number of transitions made between the states $|a\rangle$ and $|b\rangle$. The control mechanism is identified by the set of pathways $(a \rightarrow l_1 \cdots \rightarrow l_{n-1} \rightarrow b)$ connecting states $|a\rangle$ and $|b\rangle$ which have amplitudes of significant magnitude $|U_{ba}^{n(l_1,l_2,\ldots,l_{n-1})}|$. An understanding of the mechanism involves an analysis of the constructive and destructive interferences among the significant complex amplitudes $\{U_{ba}^{n(l_1,l_2,\ldots,l_{n-1})}\}$.

The integrals in Eq. (3) are computationally difficult to evaluate directly. The HE technique circumvents the direct evaluation of the integrals by solving a systematically designed sequence of Schrödinger equations related to the original Eq. (1). The basic operation in HE is the introduction of a new dimensionless timelike variable s, which is used to label the modulation (encoding) of individual matrix elements of the Hamiltonian with suitable functions $\{m_{lq}(s)\}$ of s, such that

$$h_{lq}(t) \rightarrow h_{lq}(t) m_{lq}(s). \qquad (6)$$

Integrating the new encoded equation, of the same form as Eq. (1), gives $U_{ba}(T,s)$ as a function of s, denoted as $U_{ba}(s)$ where T is omitted for notational simplicity. From the structure of Eqs. (4)–(6) it can be shown that [13]

$$U_{ba}(s) = \sum_{n=1}^\infty \sum_{l_1,l_2,\ldots,l_{n-1}=1}^d U_{ba}^{n(l_1,l_2,\ldots,l_{n-1})} M_{ba}^{n(l_1,l_2,\ldots,l_{n-1})}(s) \quad (7)$$

with

$$M_{ba}^{n(l_1,l_2,\ldots,l_{n-1})}(s) = m_{bl_{n-1}}(s) \times m_{l_{n-1}l_{n-2}}(s) \times \cdots \times m_{l_1a}(s).$$

$$(8)$$

Each transition $p \rightarrow q$ is tagged with a characteristic function $m_{pq}(s)$. This implies that the pathway $(a \rightarrow l_1 \rightarrow l_2 \rightarrow \cdots \rightarrow l_{n-1} \rightarrow b)$ is associated to the encoding tags $m_{al_1}(s), m_{l_1,l_2}(s), \ldots, m_{l_{n-1}b}(s)$, and therefore to the overall characteristic function $M_{ba}^{n(l_1,l_2,\ldots,l_{n-1})}(s)$. The task now reduces to finding the desired pathway amplitudes $U_{ba}^{n(l_1,l_2,\ldots,l_{n-1})}$ by extracting the components of $U_{ba}(s)$ associated with each basis function $M_{ba}^{n(l_1,l_2,\ldots,l_{n-1})}(s)$. The criterion for choosing the encoding functions $\{m_{pq}(s)\}$ is that they produce a unique signature function $M_{ba}^{n(l_1,l_2,\ldots,l_{n-1})}(s)$ for each amplitude $U_{ba}^{n(l_1,l_2,\ldots,l_{n-1})}$ in Eq. (8). Many choices of encoding functions $\{m_{pq}(s)\}$ will satisfy this criterion, however, complex exponentials $m_{pq}(s) = \exp(i\gamma_{pq}s)$ are simple and attractive. Complex exponentials form a set of orthogonal functions, and products of complex exponentials in Eq. (8) yield other complex exponentials. Each function in Eq. (8) becomes

$$M_{ba}^{n(l_1,l_2,\ldots,l_{n-1})}(s) = \exp\{is\,\gamma_{bl_{n-1}}\} \times \exp\{is\,\gamma_{l_{n-1}l_{n-2}}\}$$
$$\times \cdots \times \exp\{is\,\gamma_{l_1 a}\}$$
$$= \exp\{is\,\gamma^{n(l_1,l_2,\ldots,l_{n-1})}\}. \qquad (9)$$

By an appropriate choice of the dimensionless real frequencies $\{\gamma_{ij}\}$, it is possible to ensure that each distinct pathway (with some exceptions [13]) oscillates at a unique frequency $\gamma^{n(l_1,l_2,\ldots,l_{n-1})}$ as s is scanned. The extraction of the pathway amplitudes requires solving Schrödinger's equation for $U_{ba}(s)$ over a sufficient number of s points to permit performing a Fourier transform of $U_{ba}(s)$. The resultant amplitude of the spectral line at the frequency $\gamma^{n(l_1,l_2,\ldots,l_{n-1})}$ may be quantitatively identified as $U_{ba}^{n(l_1,l_2,\ldots,l_{n-1})}$.

In some cases the total number of pathways connecting the initial and final states can become very large, and the number of solutions of Schrödinger's equation needed for extracting the amplitude of each individual pathway will become correspondingly large. This is typically the case at high field intensities. In such cases by a suitable choice of the frequencies $\{\gamma_{pq}\}$ it is possible to attain a reduced mechanism by combining pathways into well defined physical pathway classes, and thereby find the net contribution of each pathway class rather than the contribution of each individual pathway. For example, the simplest choice $\gamma_{pq} = \gamma \ \forall p,q$ collects all pathways of the same order together independent of the particular intermediate transitions involved. This choice of frequencies gives an estimate of the number of photons involved in producing the overall transfer, and the relative importance of the different orders of perturbation in the population transfer. Finding the relevant orders of perturbation contributing to the dynamics provides a quick snapshot of the mechanistic complexity of the dynamics. This pathway class will be exploited in this work, although other classes of pathways (e.g., composite pathways [13–15]) could be used as well.

III. CHOICE OF REPRESENTATION AS AN OPTIMIZATION PROBLEM

A. General formalism

Mechanism identification by HE has been utilized to understand the dynamics of controlled quantum mechanical systems [13–16], where "mechanism" is taken to be a knowledge of the significant pathways connecting an initial and final state, along with their associated amplitudes. Its implementation requires a choice of representation or set of basis states, as pathways are described in terms of transitions between these basis states. In previous work the wave function was expressed in terms of the eigenstates of the field-free Hamiltonian in the interaction representation [13–15], or in terms of the "dressed states" of the system with the interacting field [14]. The revealed perspectives on the mechanism can differ vastly from one representation to another [14]. This is not a matter of right or wrong, as mechanism will always be understood in terms of some chosen reference (i.e., representation) for comparative analysis. Therefore, mechanism analysis of controlled dynamics involves two distinct steps: (i) choosing a basis to represent the system

and (ii) finding the mechanism in that representation. This section starts with the Hamiltonian in an arbitrary representation and develops a framework for identifying a new representation where the dynamics (and hence the mechanism) is simpler, as characterized by a quantitative measure of complexity.

Consider a system evolving under the Schrödinger equation (1). Once a choice of basis states $\{|1\rangle, |2\rangle, \ldots, |d\rangle\}$ has been made, the operators $H(t)$ and $U(t)$ can be represented as time varying $d \times d$ square matrices with elements $H_{lm}(t) = \langle l|H(t)|m\rangle$ and $U_{lm}(t) = \langle l|U(t)|m\rangle$. We assume that this choice of basis is physically well understood (e.g., the eigenstates of the field-free, time independent Hamiltonian H_0). Now consider a change of representation to a new set of basis states $\{|\phi_1(t)\rangle, |\phi_2(t)\rangle, \ldots, |\phi_d(t)\rangle\}$, where the t indicates that these basis states may, in general, be functions of time. This change of representation corresponds to a time varying unitary transformation $R(t)$ of the original system with the elements of $R(t)$ given by $R_{lm}(t) = \langle \phi_l(t)|m\rangle$.

The dynamical equation for the time evolution operator W_R in this representation is

$$\frac{dW_R}{dt} = -i[R(t)H(t)R^\dagger(t) + i\dot{R}(t)R^\dagger(t)]W_R(t), \qquad (10)$$

where the overdot implies a time derivative. Therefore the matrix form of the Hamiltonian in this new representation is related to the old representation by the equation

$$H_R(t) = R(t)H(t)R^\dagger(t) + i\dot{R}(t)R^\dagger(t). \qquad (11)$$

The time evolution operator $U(t)$ in the old representation is related to $W_R(t)$ by the equation $U(t) = R^\dagger(t)W_R(t)R(0)$. All transformations considered in this work shall use $R(0) = I$, therefore the equation becomes

$$U(t) = R^\dagger(t)W_R(t). \qquad (12)$$

In the case that $R(t) = U^\dagger(t)$, then we have $W_R(t) = I$. Inserting $R(t) = U^\dagger(t)$ into Eq. (11) gives $H_R(t) \equiv 0$. Therefore, in this limiting case all the dynamical complexity has been absorbed into the change of representation, leading to a dynamical equation for W_R in Eq. (10) that is trivial. At the other extreme, the original dynamics correspond to $R(t) = I$ and $W_R = U$. A familiar choice is $R(t) = \exp(iH_0 t)$ for a Hamiltonian of the general form $H = H_0 + V(t)$, where H_0 is time dependent and $V(t)$ is an external potential (e.g., a control term). In this case $H_R(t) = R(t)V(t)R^\dagger(t)$ from Eq. (11), which is the standard interaction representation.

From the viewpoint of Eq. (12), the choice of an optimal representation involves balancing a tradeoff between the complexity of $R(t)$ and $W_R(t)$. Two natural extremes may be considered: (i) a representation where the basis $\{|l\rangle\}$ is well understood, $W_R = U$ and $R(t) = I$, but the dynamics of W_R can be complex and (ii) a representation where the basis $\{U^\dagger(t)|l\rangle\}$ can be difficult to interpret but with trivial new dynamics $W_R(t) = I$. In (i) $W_R = U$ holds all the dynamics and in (ii) $R = U^\dagger$ does. Both systems provide the same level of dynamical complexity expressed in terms of U. This section develops a formalism to strike a balance between the two extremes, thus providing an opportunity for finding a repre-

sentation which is not too difficult to interpret, yet the dynamical complexity is reduced. This paper provides a systematic means to determine different forms for $R(t)$ with the mechanism understood to lie in $W_R(t)$. However, from another perspective, the original, complex mechanism residing in $U(t)$ is now dispersed between $R^\dagger(t)$ and $W_R(t)$ in Eq. (12).

Most quantum dynamics studies are performed in representations that are "well understood," implying that the basis states have a clear meaning (e.g., the eigenstates of the operator H_0). Both time-independent and time varying states have been considered. For instance, in the dressed-state representation, given a time varying Hamiltonian $H(t)$, the system is rotated by $R(t)$ such that $R(t)H(t)R^\dagger(t)$ is diagonal. In situations where $\dot{R}R^\dagger$ is negligible, the Hamiltonian, being diagonal, permits a significant simplification of the dynamics, as there are no transitions between the basis states in such a representation. Mechanism analysis in the dressed state picture was studied previously [14]. While the dressed state picture is not always appropriate, it illustrates the concept of moving to a better set of basis states to understand the dynamics. A key goal in changing the basis is to "understand" the new basis states. As dressed states have been exploited extensively, the use of such basis states is now readily accepted, with an understanding of the states coming from familiarity. In this work we shall introduce the concept of picking basis states with some degree of "optimality" and setting up the choice of a suitable transformation $R(t)$ as an optimization problem. The notion of "understanding" the new basis states shall subsequently be addressed by restricting the choice of representations to classes that are amenable to interpretation. However, additional work and exploration into flexible representations will surely be needed to attain a good level of understanding.

Consider now the formulation for deducing an optimal transformation. In general, given the Hamiltonian $H(t)$ in an initial suboptimal representation, we define the functional J

$$J = C(R,\dot{R},H) + kD(R,\dot{R}). \tag{13}$$

Here C is a functional that measures the mechanistic complexity of the dynamics after applying a transformation $R(t)$, and D is a functional that measures the complexity of the transformation; k is a heuristically determined weight, with low values corresponding to an emphasis on minimizing the dynamical complexity, and high values corresponding to an emphasis on using simple transformations. The goal is to find the transformation $R(t)$ that minimizes this cost functional. In this paper we shall utilize the specific cost function

$$J[R(t),\dot{R}(t)] = \int_0^T \{\|H_R(t)\|^2 + k\|\dot{R}(t)\|^2\}dt, \tag{14}$$

where the first term is a special case of $C(R,\dot{R},H)$, expressed as the integrated norm squared of the Hamiltonian transformed under $R(t)$ in Eq. (11). The second term is a particular choice for $D(R,\dot{R})$ that seeks to minimize the norm of the rate of variation of $R(t)$. The most appropriate measure of dynamical mechanism complexity would be obtained from identifying the highest contributing pathway order in the new

representation. However, using such a measure would be a computationally intensive task. In order to achieve the goal of minimizing Eq. (13) in a practical fashion it is important that C not actually require an explicit knowledge of the mechanism. While subsequent results show that the norm of $H_R(t)$ is only an approximate measure of dynamical mechanism complexity, it is sufficient to set up simple optimization schemes to determine transformations $R(t)$ that permit capturing all or part of the dynamics in the representation as desired. The Frobenius norm $\|A\|^2 = \Sigma_{l,m}|a_{lm}|^2 = \mathrm{Tr}(AA^\dagger)$ will be utilized in this work. While this will be the norm of choice, other choices could be utilized, for example, minimizing the norm of all off-diagonal elements instead of the entire matrix (as the diagonal elements do not induce state-to-state transformations). The first term in the integrand of Eq. (14) can be expanded as

$$\mathrm{Tr}(RHR^\dagger RHR^\dagger) - i\mathrm{Tr}(RHR^\dagger R\dot{R}^\dagger)$$
$$+ i\mathrm{Tr}(\dot{R}R^\dagger RHR^\dagger) + \mathrm{Tr}(\dot{R}R^\dagger R\dot{R}^\dagger), \tag{15}$$

where the time dependence has been omitted for brevity. The first term equals $\mathrm{Tr}(H^2)$ and using the cyclic invariance of the trace operator along with $RR^\dagger = 1$ (implying $\dot{R}R^\dagger = -R\dot{R}^\dagger$), the second and third terms may be combined as $2i\mathrm{Tr}(\dot{R}HR^\dagger)$. Finally, the last term in Eq. (15) reduces to $\mathrm{Tr}(\dot{R}\dot{R}^\dagger)$. Therefore, the cost functional becomes

$$J = \int_0^T \{\mathrm{Tr}(H^2) + 2i\mathrm{Tr}(\dot{R}HR^\dagger) + (1+k)\mathrm{Tr}(\dot{R}\dot{R}^\dagger)\}dt. \tag{16}$$

The first term integrated over time is simply the norm of the original Hamiltonian and is independent of $R(t)$; therefore we shall drop it from the cost function. Writing $k' = 1+k$, we arrive at the final cost functional

$$J[R(t),\dot{R}(t)] = \int_0^T \{2i\mathrm{Tr}(\dot{R}HR^\dagger) + k'\mathrm{Tr}(\dot{R}\dot{R}^\dagger)\}dt. \tag{17}$$

In principle, this functional can be numerically minimized for a given k' to find the optimal unconstrained transformation $R(t)$. In the limiting case of $k'=1$ the variational problem is equivalent to solving the original time-dependent Schrödinger equation, since the optimal solution is $R(t) = U^\dagger(t)$. In order to obtain a practical procedure to minimize J, it is necessary to constrain $R(t)$ to obey a suitable dynamical equation of motion. There is wide freedom in utilizing constrained forms for $R(t)$, and the cases considered in this work should be viewed as a means to illustrate the variational formulation rather than necessarily an optimal choice for practical purposes. Here we will choose $R(t)$ to satisfy the equation of motion

$$\dot{R}(t) = iA[\vec{f}(t)]R(t), \tag{18}$$

where $A[\vec{f}(t)]$ is a Hermitian matrix which depends on a vector of n time dependent parameters $\vec{f}(t)$. Substituting Eq. (18) into the cost functional in Eq. (17) yields

$$J[R(t),\dot{R}(t)] = \int_0^T \{2i\mathrm{Tr}(iA[\vec{f}]RHR^\dagger)$$

$$+ k'\mathrm{Tr}(iA[\vec{f}]RR^\dagger(-iA^\dagger[\vec{f}]))\}dt$$

$$= \int_0^T \{\mathrm{Tr}(-2A[\vec{f}]RHR^\dagger) + k'\mathrm{Tr}(A^2[\vec{f}])\}dt.$$

(19)

The goal is to find the optimal vector $\vec{f}(t)$ that minimizes the cost J in Eq. (19), subject to the constraint of Eq. (18). The vector of parameters $\vec{f}(t)$ can be viewed as the "control knobs" thereby reducing the identification of the transformation $R(t)$ to a special type of optimal control problem. In order to solve the optimization problem we introduce the augmented cost functional

$$J[R(t),\dot{R}(t),\lambda(t)] = \int_0^T [-2\mathrm{Tr}(A[\vec{f}]RHR^\dagger)$$

$$+ k'\mathrm{Tr}\{A[\vec{f}]A^\dagger[\vec{f}(t)]\}$$

$$+ \mathrm{Tr}(\lambda^\dagger\{\dot{R}(t) - iA[\vec{f}]R\}$$

$$+ (\dot{R}^\dagger + iR^\dagger A[\vec{f}])\lambda)dt],$$

(20)

where $\lambda(t)$ is a Lagrange multiplier matrix. Considering the variation with respect to $R^\dagger$, we obtain

$$\delta J = \int_0^T \mathrm{Tr}\{-2ARH\delta R^\dagger + \delta\dot{R}^\dagger\lambda + i\delta R^\dagger A[\vec{f}]\lambda\}dt. \quad (21)$$

Integrating the term $\delta\dot{R}^\dagger$ by parts produces

$$\delta J = \int_0^T \mathrm{Tr}\{-2ARH\delta R^\dagger - \delta R^\dagger\dot{\lambda} + i\delta R^\dagger A\lambda\}dt + [\delta R^\dagger\lambda]_0^T.$$

(22)

Setting the variation in $\delta R^\dagger$ to zero, we obtain the differential equation for λ

$$\dot{\lambda} = -2ARH + iA\lambda \quad (23)$$

with the boundary conditions

$$[\delta R^\dagger\lambda]_0^T = 0. \quad (24)$$

We shall show later that the value of J is invariant to replacing $R(t)$ with $KR(t)$, where K is any arbitrary (constant) unitary operator. Therefore, given a solution $R(t)$, we can pick $K = R^\dagger(0)$ to ensure that $R(0) = I$. As a result, we get from Eq. (24) the conditions $R(0) = I$ and $\lambda(T) = 0$. Finally, setting the variation of each element f_l of $\vec{f}$ to zero in Eq. (20) yields the algebraic equations

$$\frac{2\delta A[\vec{f}]}{\delta f_l}RHR^\dagger - k'\frac{\delta A^2[\vec{f}]}{\delta f_l} + i\lambda^\dagger\frac{\delta A[\vec{f}]}{\delta f_l}R - iR^\dagger\frac{\delta A[\vec{f}]}{\delta f_l}\lambda = 0,$$

$$l = 1,\dots,n. \quad (25)$$

Equations (18), (23), and (25) are the working variational equations along with $R(0) = I$ and $\lambda(T) = 0$. In practical imple-

mentations of the optimization procedure it can be convenient to further constrain the transformation to a suitable functional form. Certain transformation forms can lead to equations that may be simpler to solve numerically, produce simpler interpretations, or have other helpful features without explicitly employing the general procedure developed above. The treatment that follows is an initial step in this direction.

B. Closed-form optimization for constrained changes of representation: One-point optimization procedure

There are many ways to constrain and parameterize the change of representation given by $R(t)$ based on mathematically desired properties or physical motivation. The simplest transformation would be a time independent operator R. However, this change of representation does not simplify the dynamical mechanism, as defined in Sec. II. This can be established by inserting $R(t) = R$, $\dot{R}(t) = 0$, $\forall$ t in Eq. (16) to obtain

$$J[R] = \int_0^T \mathrm{Tr}(H^2)dt, \quad (26)$$

which is exactly the cost in the original representation. Therefore, under the cost measure defined in Eq. (14), time-independent transformations will not reduce mechanistic complexity. In order to better understand this behavior, consider, for example, a typical integral in the Dyson series expansion

$$(-i)^2 \int_0^t H(t_2) \int_0^{t_2} H(t_1)dt_1 dt_2. \quad (27)$$

Under a transformation $H(t) \to RH(t)R^\dagger$ with $\dot{R} = 0$, $\forall$ t, the Frobenius norm of this integral will remain unchanged. A similar argument can be made for all other integrals in the Dyson series. Hence for time-independent transformations, the number of significant terms in the expansion for W_R cannot change, and only the dominant pathways within a given order may vary [e.g., the separate contributions within the second order terms of Eq. (27)]. Therefore, we do not further consider time independent changes of representation in this work.

A natural next step is to consider a simple time dependent transformation matrix, given by

$$R(t) = \exp[iAb(t)], \quad (28)$$

where A is a time-independent Hermitian matrix and $b(t)$ is a scalar function. Equation (28) is a special case of the general transformation embodied in Eq. (18). The structure of this constrained transformation simplifies the optimization functional allowing for closed-form equations for the optimal representation. Equation (28) is related to various approximate solutions of the Schrödinger equation. The treatment in Sec. IV will consider general representation changes as a time-ordered product of transformations of the form given in Eq. (28), valid for N successive time intervals, which in the limit of $N \to \infty$ gives an unconstrained form for the change of representation.

From Eq. (28), $\dot{R}=iA\dot{b}R$, and substitution into Eq. (17) gives

$$J[\dot{b}(t),A] = \int_0^T \{2i\text{Tr}[iA\dot{b}(t)RHR^\dagger]$$

$$+ k'\text{Tr}[iA\dot{b}(t)RR^\dagger(-i)A^\dagger\dot{b}(t)]\}dt. \quad (29)$$

The form of $R(t)$ in Eq. (28) implies that R commutes with A at all times, thereby reducing J to

$$J[\dot{b}(t),A] = \int_0^T \{-2\dot{b}(t)\text{Tr}[AH(t)] + k'\dot{b}(t)^2\text{Tr}(AA^\dagger)\}dt. \quad (30)$$

This is a function of A and $\dot{b}$, not $b(t)$, so $b(t)$ is only determined up to an arbitrary constant. The goal is to find A and $\dot{b}$ that minimize J in Eq. (30). First consider optimization for $\dot{b}$ by setting the first order variations in $\dot{b}$ to zero,

$$\dot{b}(t) = \frac{\text{Tr}[AH(t)]}{k'\text{Tr}(AA^\dagger)}. \quad (31)$$

Since A is Hermitian, we treat the upper half of its matrix elements a_{pq} (with $p \geq q$) as independent variables. The diagonal elements are real, while the off-diagonal are in general complex. In terms of the elements a_{pq} in the upper half of A, and similarly $h_{pq}(t)$ of $H(t)$, the cost function becomes

$$J = \int_0^T \left\{ -2\dot{b}(t)\left[\sum_p a_{pp}h_{pp}(t) + \sum_{p,q>p} a_{pq}h_{qp}(t) + \text{c.c.}\right] \right.$$

$$\left. + k'\dot{b}(t)^2\left[\sum_p a_{pp}a_{pp} + 2\sum_{p,q>p} a_{pq}a_{pq}^*\right]\right\}dt. \quad (32)$$

Setting the partial derivatives of each of the independent variables a_{pq} of A to zero yields

$$A = \frac{\displaystyle\int_0^T \dot{b}(t)H(t)dt,}{\displaystyle\int_0^T k'\dot{b}(t)^2dt.} \quad (33)$$

The system of equations given by Eqs. (31) and (33) can be solved by iteration to find $\dot{b}(t)$ and A.

Consider now an arbitrary unitary matrix K used to replace $R(t)$ in Eq. (17) with $KR(t)$ to obtain

$$J[KR(t),K\dot{R}(t)] = \int_0^T \{2i\text{Tr}(iKRHR^\dagger K^\dagger) + k'\text{Tr}[K\dot{R}\dot{R}^\dagger K^\dagger]\}dt. \quad (34)$$

Using the cyclic invariance of the trace operator and $KK^\dagger=I$, it follows that J is invariant to K. Therefore, if J is optimized for $\exp[iAb(t)]$, it will also be optimized for $K\exp[iAb(t)]$. Replacing $b(t)$ with $b(t)+c$, where c is constant, is a special case of $K=\exp(icA)$, which leaves the cost J unchanged. Therefore, $b(t)$ is only determined up to an arbitrary constant which can be chosen as $b(0)=0$, in keeping with $R(0)=I$. The new representation therefore coincides

with the original one at $t=0$. We also note that if A and $b(t)$ optimize J, then A/c' and $c'b(t)$ for any real constant $c' \neq 0$ is also a solution. The results are normalized by setting the maximum value of $\dot{b}$ to $1/k'$.

In the case of $k'=1$ or $k=0$ the optimization goal in Eq. (14) is to find the transformation which minimizes the norm of $H_R(t)$. As shown earlier, the unconstrained representation $R(t)$ that minimizes the norm of $H_R(t)$ is $U^\dagger(t)$. Minimizing the cost in Eq. (30) corresponds to finding $R(t)$ of the form $\exp[iAb(t)]$ which is the best approximation to $U^\dagger(t)$. Equivalently $R^\dagger(t)$ will be the closest approximation to $U(t)$, capturing the dynamics induced by the Hamiltonian in the original representation. Also, if A and $b(t)$ optimize J for $k'=1$, then A and $b(t)/k'$ optimize J for all other values of k'. Therefore, solving the optimization problem for $k'=1$ automatically generates the solution for all other values of k'.

The interpretation of the transformation $R(t)$ can be seen from the following special case where the Hamiltonian has the form $H(t)=g(t)H'$. Then the time evolution is given by

$$U(t) = \exp\left[-iH'\int_0^t g(u)du\right], \quad (35)$$

which exactly matches $R^\dagger(t)$ with $H'=A$ and $g(t)=\dot{b}(t)$. This result may be verified by observing that $A=H'$ and $\dot{b}(t)=g(t)$ satisfy Eqs. (31) and (33). Hamiltonians of this simple form can arise in the context of controlled systems governed by the rotating wave approximation (RWA). Consider a system of the form

$$H = H_0 - \mu\mathcal{E}(t), \quad (36)$$

where H_0 is the field free Hamiltonian, μ is the dipole operator, and $\mathcal{E}(t)$ is the control field. In the interaction representation, the time evolution becomes

$$\frac{dU}{dt} = -i[\mu_I(t)\mathcal{E}(t)]U \quad (37)$$

with $\mu_I(t)=\exp(iH_0t)\mu\exp(-iH_0t)$. As a special case, we consider systems where the control field is of the form

$$\mathcal{E}(t) = 2g(t)\sum_{l=1}^d\sum_{m=1}^l b_{lm}\cos(\omega_{lm}t + \phi_{lm}), \quad (38)$$

where $g(t)$ is a slowly varying envelope function over the range $[0, 1]$, and each frequency ω_{lm} is resonant with only one transition $|l\rangle \rightarrow |m\rangle$. Then in the RWA [18], the time evolution becomes

$$\frac{dU}{dt} = -i\mu g(t)U. \quad (39)$$

In practice, when such a system is propagated using the interaction equation [Eq. (37)], although the long term dynamics follows the RWA, there are significant short term fluctuations which are lost. The short term fluctuations can be removed by the smoothing procedure of replacing $H(t)$ by its average value over an interval $[t-\delta/2, t+\delta/2]$. This smoothing procedure acts as a low pass filter on $H(t)$, characterized

by the small parameter δ, that removes the short term fluctuations.

C. Closed-form optimization for constrained changes of representation: Two-point optimization procedure

HE seeks to understand the mechanism induced by the control $\mathcal{E}(t)$ acting over a time interval $[0,T]$. For example, in the original representation, one may consider two basis states, say $|a\rangle$ and $|b\rangle$, and subject the element $U_{ba}(T)$ to mechanism analysis. After making a representation change, transitions occur between basis states $|\phi_a\rangle$ and $|\phi_b\rangle$, which are given by $R^{\dagger}(t)|a\rangle$ and $R^{\dagger}(t)|b\rangle$, and then a mechanism analysis would be performed on $W_{\phi_b,\phi_a}(T)$. While the new basis states coincide with $|a\rangle$ and $|b\rangle$ at $t=0$, in general they will be different states at $t=T$. However, despite the representation change, we may still desire to analyze the mechanism between the states $|a\rangle$ and $|b\rangle$. In this case we may introduce a new, optimal representation which is constrained to match the original representation at times 0 and T [i.e., $R(0)=R(T)=I$]. Then $|a\rangle$ and $|b\rangle$ will remain as the basis states at both the initial and final times, and from Eq. (12) $W_{\phi_b,\phi_a}(T) \equiv U_{ba}(T)$, although the mechanism will reflect the presence of the change of representation. For the constrained case of Eq. (28), this corresponds to optimizing the cost functional in Eq. (30) with the constraints $b(0)=b(T)=0$, or equivalently, optimizing the augmented cost functional

$$J_A = \int_0^T \{-2\dot{b}(t)\text{Tr}[AH(t)] + k'\dot{b}(t)^2\text{Tr}(AA^{\dagger})\}dt$$
$$+ \lambda_1 b(0) + \lambda_2 b(T). \tag{40}$$

Setting the variations in b to be zero

$$0 = \int_0^T \{-2\,\delta\dot{b}(t)\text{Tr}[AH(t)] + 2k'\,\delta\dot{b}(t)\dot{b}(t)\text{Tr}(AA^{\dagger})\}dt$$
$$+ \lambda_1\delta b(0) + \lambda_2\delta b(T) \tag{41}$$

and integrating by parts yields

$$0 = \int_0^T \{2\,\delta b(t)\text{Tr}[A\dot{H}(t)] - 2k'\,\delta b(t)\ddot{b}(t)\text{Tr}(AA^{\dagger})\}dt$$
$$+ \{2\,\delta b(t)\text{Tr}[AH(t)]\}_0^T + [2k'\,\delta b(t)\dot{b}(t)\text{Tr}(AA')]_0^T$$
$$+ \lambda_1\delta b(0) + \lambda_2\delta b(T). \tag{42}$$

The boundary terms can be used to compute the values of the Lagrange multipliers λ_1 and λ_2, but their values are not important here. From Eq. (42), $b(t)$ satisfies

$$\text{Tr}[A\dot{H}(t)] - k'\ddot{b}(t)\text{Tr}(AA^{\dagger}) = 0, \tag{43}$$

which may be solved with the boundary conditions $b(0)=b(T)=0$ to give

$$b(t) = \frac{1}{k'\text{Tr}(AA^{\dagger})}\left[\int_0^t \text{Tr}[AH(\tau)]d\tau - ct\right] \tag{44}$$

with

$$c = \frac{1}{T}\int_0^T \text{Tr}[AH(\tau)]d\tau. \tag{45}$$

The optimization for A, given $b(t)$ in Eq. (44), remains exactly the same as before, producing Eq. (33). This particular form of the optimization problem shall be referred to later as the two-point optimization procedure.

IV. GENERALIZED REPRESENTATION CHANGES

The previous section developed an optimization procedure to find a quantum-mechanical representation. We now present two flexible generalizations that go beyond the constrained transformation $R(t)=\exp[iAb(t)]$ in Eq. (28). The first procedure involves dividing the Hamiltonian into smaller time intervals and optimizing the representation for each time piece separately, and is referred to as optimization by time division. The second approach involves iteratively repeating the procedure of Sec. III until the desired representation is achieved. This is referred to as optimization by iteration.

A. Optimization by time division

The first generalization of the procedure of Sec. III involves dividing $H(t)$ into time intervals and applying the optimization procedure based on the constrained form of Eq. (28) to each individual interval. First consider dividing $H(t)$ over a time interval $[0,T]$ into two parts $H_1(t)=H(t)$ for $t \in [0,T/2]$, $H_1(t)=0$ otherwise, and $H_2(t)=H(t)$ for $t \in [T/2,T]$, $H_2(t)=0$ otherwise. Then we use the optimizing equations [Eqs. (31) and (33)] for $H_1(t)$ over the interval $[0,T/2]$ to get A_1 and $\dot{b}_1(t)$ as

$$\dot{b}_1(t) = \frac{\text{Tr}[A_1 H(t)]}{k'\text{Tr}(A_1^2)} \quad \text{for } t \in [0,T/2] \tag{46}$$

and

$$A_1 = \frac{\int_0^{T/2}\dot{b}_1(t)H(t)dt}{\int_0^{T/2}k'\dot{b}_1(t)^2}. \tag{47}$$

Applying the same procedure for $H_2(t)$ over the interval $[T/2,T]$ gives

$$\dot{b}_2(t) = \frac{\text{Tr}[A_2 H(t)]}{k'\text{Tr}(A_2^2)} \quad \text{for } t \in [T/2,T] \tag{48}$$

and

$$A_2 = \frac{\int_{T/2}^0 \dot{b}_2(t)H(t)dt}{\int_{T/2}^T k'\dot{b}_2(t)^2}. \tag{49}$$

These equations are solved with the respective initial conditions $b_1(0)=0$ and $b_2(T/2)=0$. Then the overall transformation to use for $H(t)$ is $R_1(t)=\exp[iA_1 b_1(t)]$ for $t \in [0,T/2]$, and $R_2(t)=\exp[iA_2 b_2(t)]$ for $t \in [T/2,T]$. However, Sec. III

showed that $R_2(t) = K \exp[iA_2 b_2(t)]$ would also be an optimal solution over the range $[T/2, T]$ for any arbitrary unitary K. Therefore, to ensure that $R(t)$ is continuous over the whole range $[0, T]$, we choose $K = \exp[iA_1 b_1(T/2)]$ and write $R_2(t) = \exp[iA_1 b_1(T/2)]\exp[iA_2 b_2(t)]$, which will guarantee continuity such that $R_1(T/2) = R_2(T/2)$.

This procedure may be generalized in a simple fashion. If the control is nonzero over the time interval $[0, T]$ then

we divide the interval T into P parts: $[0, T/P]$, $[T/P, 2T/P], \ldots, [(P-1)T/P, T]$ and perform the optimization of Sec. III on each of the separate Hamiltonian pieces. This will generate the sets $\{A_i\}$ and $\{b_i(t)\}$ for each of the corresponding sub-Hamiltonians, with the initial conditions $b_i[(i-1)T/P] = 0$, $i = 1, 2, \ldots, P$. Then $R(t)$ will be continuous on $[0, T]$ and composed from these individual transformations as

$$R(t) = \begin{cases} \exp[iA_1 b_1(t)] \text{ for } t \in [0, T/P], \\ \exp[iA_1 b_1(T/P)]\exp[iA_2 b_2(t)] \text{ for } t \in [T/P, 2T/P], \\ \exp[iA_1 b_1(T/P)]\exp[iA_2 b_2(2T/P)]\exp[iA_3 b_3(t)] \text{ for } t \in [2T/P, 3T/P], \\ \cdots, \\ \exp[iA_1 b_1(T/P)] \cdots \exp[iA_{P-1} b_{P-1}(P-1)T/T]\exp[iA_P b_P(t)] \text{ for } t \in [(P-1)T/P, T]. \end{cases} \quad (50)$$

In this case $R^\dagger(T)$ can be viewed as arising from the dynamics induced by evolution under a Hamiltonian given by

$$\mathcal{H}_R(t) = \begin{cases} A_1 \dot{b}_1(t) \text{ for } t \in [0, T/P], \\ A_2 \dot{b}_2(t) \text{ for } t \in [T/P, 2T/P], \\ \cdots, \\ A_P \dot{b}_P(t) \text{ for } t \in [(P-1)T/P, T]. \end{cases} \quad (51)$$

In practice this procedure may be stopped at any value of $P \geq 1$, and the goal is to seek a transformation that reduces the complexity of the mechanism in $W_R(T)$ to an acceptable level. Notwithstanding this goal, in the limit of $P \to \infty$, the original Hamiltonian $H(t)$ will be broken into an infinite number of time intervals with time-independent sub-Hamiltonians, in which the dynamics can be perfectly captured by $\exp[iAb(t)]$ with $b(t)$ being linear in time. For $k' = 1$ the procedure yields a $R(t)$ which is a time-ordered product of transformations that should converge to $U^\dagger(t)$ as $P \to \infty$, corresponding to one of the standard numerical procedures for solving the Schrödinger equation. This behavior makes clear how any choice for P will strike a managed balance in transforming some of the dynamics into the system representation R with the remainder residing in W_R.

B. Optimization by iteration

This section develops an alternative generalization of the procedure of Sec. III. Instead of dividing the Hamiltonian into time intervals, the Hamiltonian in the current representation is iteratively taken as input into the next level of the optimization procedure. Consider the new Hamiltonian $H_1(t)$ generated by applying $R_1(t) = \exp[iA_1 b_1(t)]$ on the original Hamiltonian $H(t)$, where A_1 and $b_1(t)$ would be obtained by solving Eq. (31) and (33) for $H(t)$

$$H_1(t) = R_1 H R_1^\dagger + i \dot{R}_1 R_1^\dagger. \quad (52)$$

Now starting with $H_1(t)$, we apply the same optimization procedure to generate $R_2(t) = \exp[iA_2 b_2(t)]$ by solving Eqs. (31) and (33) for $H_1(t)$, forming

$$H_2(t) = R_2 H_1 R_2^\dagger + i \dot{R}_2 R_2^\dagger. \quad (53)$$

Inserting $H_1(t)$ [Eq. (52)] in the above expression gives

$$\begin{aligned} H_2(t) &= R_2[R_1 H_0 R_1^\dagger + i\dot{R}_1 \dot{R}_1^\dagger]R_2^\dagger + i\dot{R}_2 R_2^\dagger \\ &= R_2 R_1 H_0 R_1^\dagger R_2^\dagger + iR_2 \dot{R}_1 R_1^\dagger R_2^\dagger + i\dot{R}_2 R_1 R_1^\dagger R_2^\dagger, \quad (54) \end{aligned}$$

where the identity operator $R_1(t)R_1^\dagger(t)$ has been inserted in the last term. Finally, this expression can be rewritten as

$$H_2(t) = R_2 R_1 H_0 R_1^\dagger R_2^\dagger + i\frac{d}{dt}[R_2 R_1]R_1^\dagger R_2^\dagger, \quad (55)$$

which corresponds to applying the transformation $R_2(t)R_1(t) = \exp[iA_2 b_2(t)]\exp[iA_1 b_1(t)]$ on the Hamiltonian $H(t)$ in the original representation. $H_2(t)$ can similarly be transformed again, and this process extended iteratively as often as desired, generating a sequence of representations for the Hamiltonian $\{H_n(t)\}$.

This iterative procedure can be naturally extended to the two point optimal representation case of Sec. III C, where the initial and final transformation are constrained to be the identity. For example, if $R_1(0) = R_1(T) = R_2(0) = R_2(T) = I$, then the composition of two transformations $R_2(t)R_1(t)$ also satisfies $R_2(0)R_1(0) = R_2(T)R_1(T) = I$. Hence the two point optimization can also be iterated.

The two generalizations developed in this section allow for effectively choosing optimal rotations for general systems, where the control field is not constrained to fit any functional form. The trade off between complexity in representation and mechanism was made in the choice of P or N, the number of time divisions and iterations, respectively.

Finally, an analysis of Eqs. (31) and (33) shows that they will generally not be satisfied by the interaction representation transformation $R(t)=\exp(iH_0t)$ for a Hamiltonian of the form of Eq. (36). This behavior points out the distinction between seeking a transformation for mechanism simplification versus that of isolating the dynamics of the external field in the standard interaction representation.

V. NUMERICAL ILLUSTRATIONS

This section illustrates the formalism developed in Secs. III and IV on several numerical examples. We first consider simple systems whose dynamics are fully captured by transformations of the form $\exp[iAb(t)]$ as an initial testing ground and means to present the concepts before considering more general systems. In all cases where HE is employed to reveal the mechanism, the modulation is applied to the elements of the transformed Hamiltonian $H_R(t)$ in Eq. (11) following the procedure of Sec. II to reveal the mechanism of the transformed time evolution in Eq. (10).

A. Systems within the RWA

The first illustration is a four-level system A with Hamiltonian of the form $H(t)=g(t)H'$, where $H'=\Sigma_{k\neq l}h'_{kl}|k\rangle\langle l|$ with $h'_{12}=1.653$, $h'_{13}=1.054$, $h'_{14}=1.600$, $h'_{23}=0.914$, $h'_{24}=0$ and $h'_{34}=0.790$ $(h'_{ji}=h'_{ij})$ and $g(t)=2\exp[-(t-500)^2/150^2]$. The dynamics are followed from $t=0$ to $T=1000$ (the results of all the examples are expressed in arbitrary dimensionless units). For system A, the time evolution is exactly expressed by Eq. (35), and as expected, the optimization procedure of Sec. III with $k'=1$ exactly identified $R(t)=U^\dagger(t)$. As a numerical test, the cost functional J of Eq. (30) in the original representation $R(t)\equiv I$ is 17.9, and the cost function was reduced to 1.2×10^{-7} after minimization. The numerically determined function $\dot{b}(t)$ was essentially identical to $g(t)$ (not shown here). Thus, $R(t)$ is a representation that rotates the system such that the norm of $H(t)$ is essentially zero.

This simple example clearly illustrates the interpretation of the transformation $R(t)=\exp[iAb(t)]$ as the dynamics of a quantum system with the Hamiltonian $\mathcal{H}_R=-A\dot{b}(t)$. The transformation $R(t)$ can be understood as the dynamics of this simple Hamiltonian, and the time evolution operator in the new transformation $W_R(t)$ and its associated mechanism can be viewed as the deviation from the dynamics of the simplified Hamiltonian. In this particular case $H_R(t)=0$ and $W_R(t)=I$, resulting in a trivial mechanism, as expected, since the representation captures the full dynamics of the system. In general, the optimization routine aims to generate a (simple) Hamiltonian $\mathcal{H}_R$ which produces the best match for the underlying system dynamics. k' can be interpreted as a limiting factor on the dynamical complexity that the optimization routine is permitted to use. For $k'=1$ (no cost on the dynamics of the transformed system), the optimization seeks the $\mathcal{H}_R$ that generates the closest match to the system dynamics.

As a second illustration we generate system B, a four level system with the Hamiltonian $H=H_0-\mu\mathcal{E}(t)$, where $H_0=\Sigma_iE_i|i\rangle\langle i|$ with $E_1=0$, $E_2=0.811$, $E_3=3.026$,
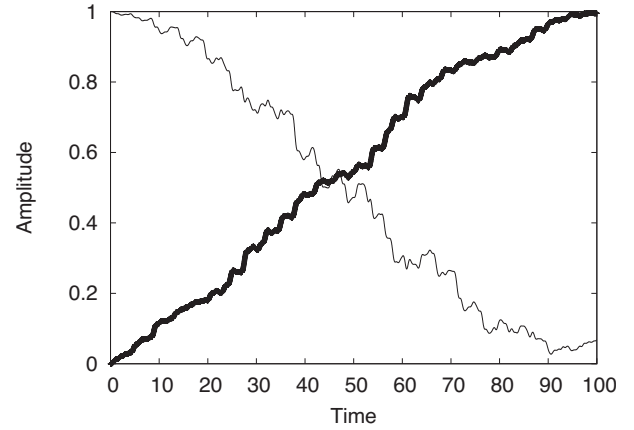
FIG. 1. $|U_{11}(t)|$ and $|U_{31}(t)|$ for the optimally controlled system C. The optimal control target was to maximize $|U_{31}(T)|^2$ at $T=100$.

$E_4=10.534$, and $\mu=H'$ of system A. The control field is $\mathcal{E}(t)=0.1\exp[-(t-500)^2/150^2]\Sigma\cos(\omega_{lm}t)$, where $\omega_{lm}=(E_l-E_m)$. This system satisfies the RWA rather well (not shown here). The norm J of the original Hamiltonian $H(t)$ with $k'=1$ in Eq. (14) was found to be 0.70, and upon transformation by the optimal representation procedure of Sec. III to $H_R(t)$, the norm was reduced to 0.47. In this case the change of basis has a modest effect as measured by the norm of the original and transformed Hamiltonians. It was found that the value of the norms can be reduced by the filtering method discussed in Sec. III. The desired population transfer ($|1\rangle\rightarrow|4\rangle$) in this case is little influenced by reasonable filtering with δ up to 100 for $T=1000$, as the system B satisfies the RWA. The example also illustrates that the Hamiltonian norm J is not a perfect measure of transformation performance. However, further examples will illustrate that minimization of J can nevertheless be very effective.

B. More general systems

We now consider Hamiltonians where the RWA is generally not valid, and the control field is of free form, determined by optimal control theory [1] without the constrained form of Eq. (38). Consider the new system C, whose parameters are chosen as $E_1=0$, $E_2=1.711$, $E_3=3.026$, $E_4=4.134$ and $\mu_{12}=1.653$, $\mu_{13}=0.254$, $\mu_{14}=1.5$, $\mu_{23}=0.814$, $\mu_{24}=0.025$, and $\mu_{34}=0.79$ $(\mu_{ij}=\mu_{ji})$. The optimal pulse maximized $|U_{31}(T)|^2$ at $T=100$ to produce $|1\rangle\rightarrow|3\rangle$ population transfer of 0.99. Figure 1 shows the transfer process by plotting $|U_{11}(t)|$ and $|U_{31}(t)|$, and Table I lists the amplitudes of some of the pathways contributing to the population transfer. Significant high order pathways contribute to the mechanism in the reference interaction representation of H_0. The system C was rotated into an optimal representation using Eq. (28) of Sec. III B. The reduction in norm, from $J=3.83$ to 2.98 is relatively small. In order to find more effective representations we will apply the procedures outlined in Sec. IV.

For the time division technique of Sec. IV A. Figure 2 shows the optimal value of the Hamiltonian norm J as a function of the number of time intervals P, where $P=0$

TABLE I. A portion of the mechanism for the population transfer $|1\rangle \rightarrow |3\rangle$ of the system C in the original representation. While pathways up to third order are shown here, significant higher order pathways contribute as well.

Pathway	Amplitude
$(1 \rightarrow 3)$	$-0.81 + 0.25i$
$(1 \rightarrow 2 \rightarrow 3)$	$-0.92 + 0.54i$
$(1 \rightarrow 4 \rightarrow 3)$	$-0.24 + 0.12i$
$(1 \rightarrow 2 \rightarrow 1 \rightarrow 3)$	$0.32 - 0.10$

corresponds to the initial representation ($R=I$). The Hamiltonian norm diminishes rapidly as P increases, showing that most of the dynamics is captured by $R(t)$. For $P=0$ all the complexity resides in the dynamics $U(t)$, while for $P \rightarrow \infty$ all the complexity is shifted to the representation $R(t)$. Figure 3 illustrates the new basis states $\{|\phi_n\rangle = R^\dagger(t)|n\rangle\}$, $n=1,2,3,4$ for the intermediate case of $P=16$, where $R^\dagger(t)$ has captured part of the system dynamics. The transformation components reflect complex dynamical behavior for $|\phi_n\rangle$, $n=1,2,3$. The behavior of $|\phi_4\rangle \approx |4\rangle$ indicates that this representation retains essentially the original character of state $|4\rangle$ reflecting
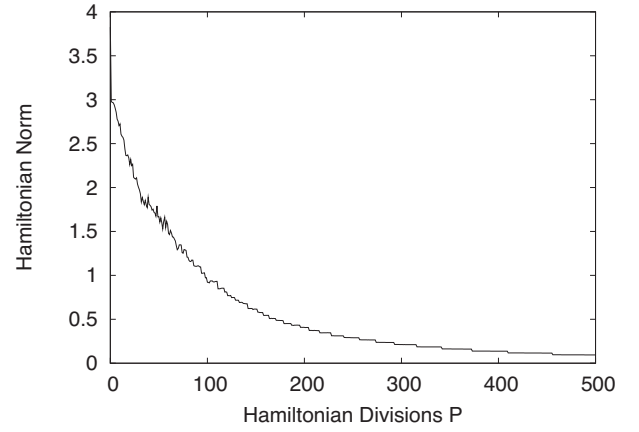
FIG. 2. Hamiltonian norm for system C as a function of the number P of intervals in which the dynamics is divided following the optimization by the time division procedure in Sec. IV A. As P increases, the complexity of the mechanism of W_R is reduced.

its reduced role in the mechanism. From another perspective, Fig. 4 presents $R^\dagger_{11}(t)$ and $R^\dagger_{31}(t)$ for the cases of $P=16$ and $P=64$, and comparison to Fig. 1, shows how the dynamics in $R^\dagger(t)$ begins to approach $U(t)$ as P increases.
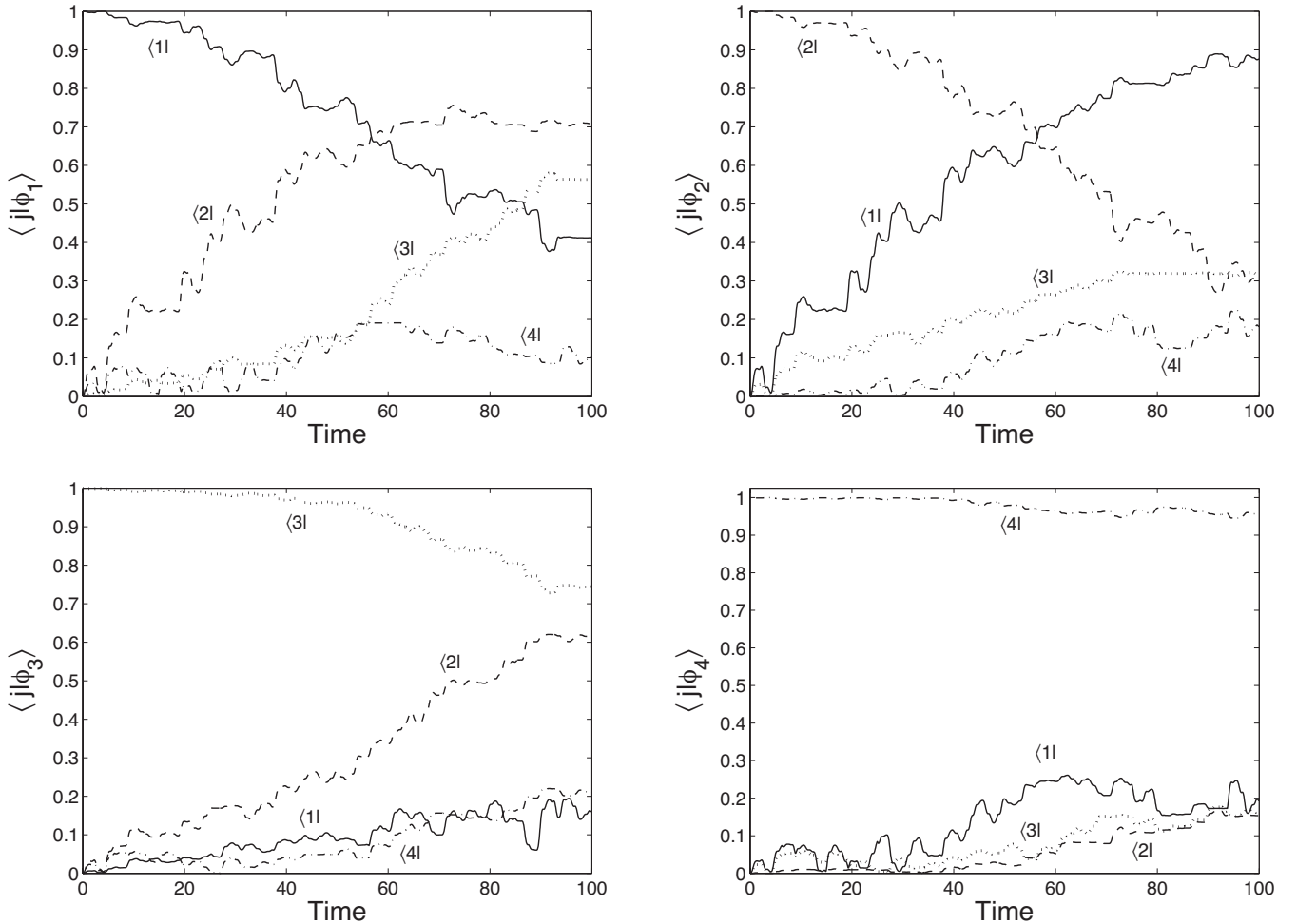
FIG. 3. $\langle j|R^\dagger(t)|i\rangle = |\phi_i\rangle$ for $i=1,2,3,4$ using the time division algorithm with $P=16$ for system C. These plots show the basis states of the new representation in terms of the eigenstates of H_0.
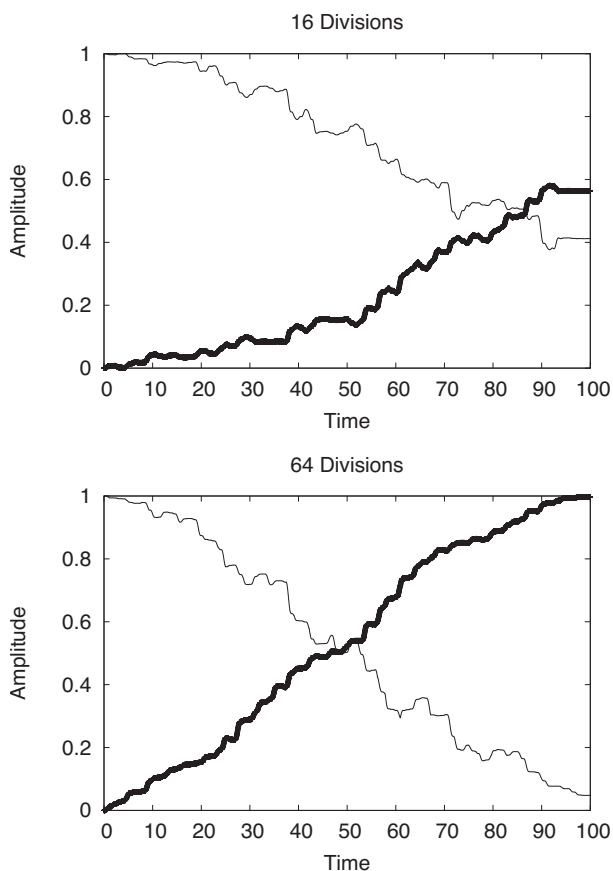
FIG. 4. $|R_{11}^\dagger(t)|$ and $|R_{31}^\dagger(t)|$ for the time division procedure, when the Hamiltonian of system C has been divided into 16 and 64 divisions. On comparing to Fig. 1, the representation begins to clearly resemble the original dynamics as P increases.

Figure 2 shows that the norm of the transformed Hamiltonian in the case $P=512$ is very small, which means that $R(t)$ has almost completely captured *all* of the dynamics. The case $P=64$ is interesting, as Fig. 2 shows that the Hamiltonian H_R has a fairly large norm, yet Fig. 4 shows that the dynamics of $R_{31}^\dagger(T)$ are very similar to that in the original representation. This result means that the remaining structure in H_R (i.e., the Hamiltonian in the transformed basis at $P=64$) does not lead to any significant dynamics. The $P=16$ case shows an intermediate situation in which the representation change has only partially captured the dynamics.

The trade off between the complexity of the representation and the complexity of the system dynamical mechanism in W_R is illustrated in Fig. 5. A mechanism analysis was done on the transformed time evolution operator $W_R(T)$, by encoding its underlying Hamiltonian H_R and Fig. 5 shows the magnitude of the amplitudes of different orders of the Dyson expansion contributing to $W_{\phi_3,\phi_1}(T)$ in the new representation. For example, the amplitude corresponding to $n=1$ is the magnitude of the contribution of the direct transition $|\phi_1\rangle \rightarrow |\phi_3\rangle$ connecting the initial state $|\phi_1\rangle$ to the final state $|\phi_3\rangle$, the second order term is the norm of the sum of the second order transitions $|\phi_1\rangle \rightarrow |\phi_2\rangle \rightarrow |\phi_3\rangle$ and $|\phi_1\rangle \rightarrow |\phi_4\rangle \rightarrow |\phi_3\rangle$, etc. As can be seen, the less complex transformation $R(t;P=16)$ leaves some higher orders moderately contributing to the transfer process. When the Hamiltonian undergoes the
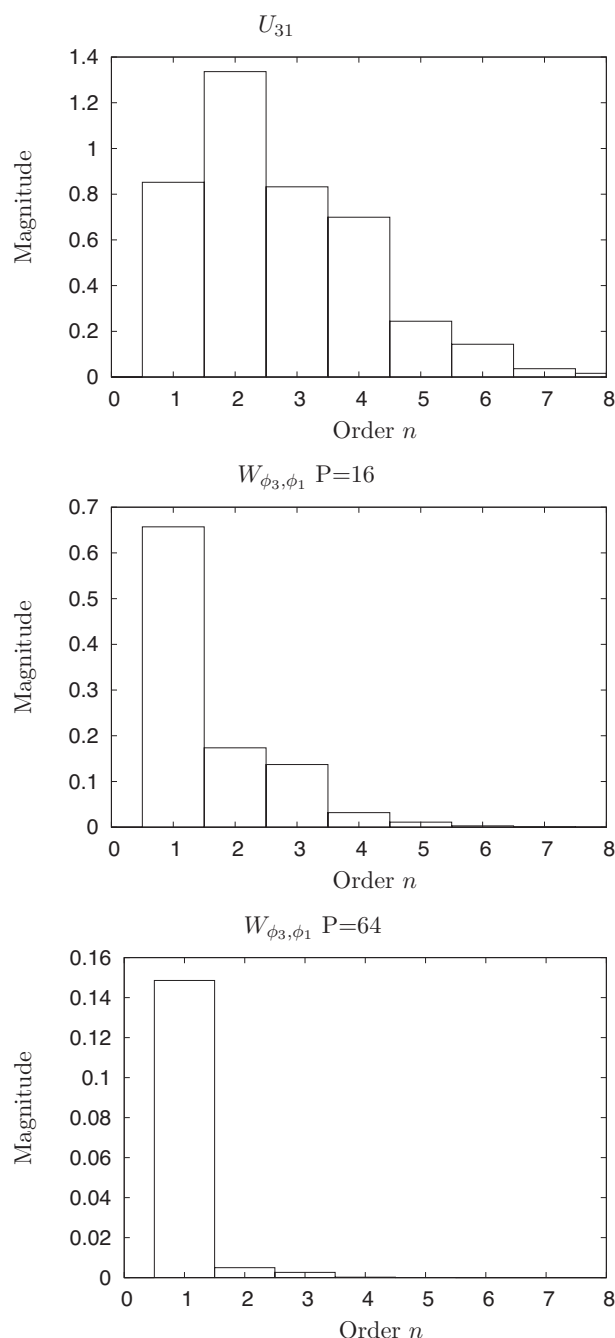
FIG. 5. This figure compares the contributions of different orders of mechanistic pathways for system C in the original representation $U_{31}(T)$ to those of W_{ϕ_3,ϕ_1} for $P=16$ and $P=64$, following the procedure in Sec. IV A. As P increases the complexity of the mechanism in W_R is reduced.

$R(t;P=64)$ transformation, the mechanism shows only first order terms.

A full HE mechanism analysis on $W_{\phi_3,\phi_1}(T)$ for the Hamiltonian in the new representations was done and the results are shown in Table II. As can be seen, there is very little dynamical behavior in the case of $P=64$, and even in the $P=16$ case, the dynamics are significantly simpler than in the original representation. Therefore, for the time division method with $k'=1$ one can choose a particular value of P

TABLE II. Comparing the mechanisms of $W_{\phi_3,\phi_1}(T)$ for system C in terms of the pathway amplitudes for two optimal representations, obtained by splitting $H(t)$ into $P=16$ and 64 parts. For $P=16$ the dynamics is already considerably simpler than in the initial representation, and for $P=64$ the dynamics is given almost totally by a small first order term.

Pathway	$W_{\phi_3,\phi_1}(T;P=16)$	$W_{\phi_3,\phi_1}(T;P=64)$
$(\phi_1 \rightarrow \phi_3)$	$-0.61+0.23i$	$-0.12+0.08i$
$(\phi_1 \rightarrow \phi_2 \rightarrow \phi_3)$	$-0.05+0.04i$	-0.01
$(\phi_1 \rightarrow \phi_4 \rightarrow \phi_3)$	$-0.09+0.04i$	0
$(\phi_1 \rightarrow \phi_2 \rightarrow \phi_1 \rightarrow \phi_3)$	$0.01-0.01i$	0.01

where the trade off between representation and mechanistic complexity is deemed appropriate. This trade off also poses the need to "understand" the representation $R(t)$, which itself can be complex. Importantly, the algorithm provides a means to systematically balance the correlated tasks of understanding mechanism captured in $W(t)$ in reference to an understanding of the representation $R(t)$.

We now consider the application of the iterative procedure of Sec. IV B on system C. Fig. 6 shows the value of the Hamiltonian norm after each iteration. As can be seen, the dynamics are effectively transferred to $R(t)$ within a few iterations and the convergence properties of this procedure are much faster than in the time-interval splitting technique. Importantly, the iteration procedure can be halted at an appropriate trade off point between the dynamical complexity in $W_R(t)$ and the representation complexity $R(t)$. Table III shows the mechanism of $W_{\phi_3,\phi_1}(T)$ in the new representation after five and eight iterations, and Fig. 7 shows the contributions of different mechanistic orders to $W_{\phi_3,\phi_1}(T)$. After five iterations the dynamics of the transformed system are almost first order, and after eight iterations, even the first order term has decreased. These two levels of iteration represent different balances between the complexity of the representation change R and the dynamics in the evolution W_R under $H_R(t)$. By 30 iterations all the dynamics is shifted to the representation and the Hamiltonian in the new representation shows
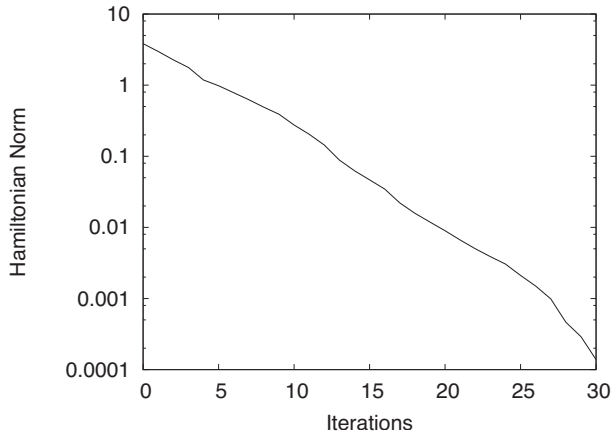
FIG. 6. Hamiltonian norm for system C as a function of the number of iterations following the optimization procedure of Sec. IV B.

TABLE III. Mechanism analysis of $W_{\phi_3,\phi_1}(T)$ for system C in two optimal representations, obtained from transformation of $H(t)$ after $N=5$ and $N=8$ iterations.

Pathway	$W_{\phi_3,\phi_1}(T;n=5)$	$W_{\phi_3,\phi_1}(T;n=8)$
$(\phi_1 \rightarrow \phi_3)$	$-0.56+0.24i$	$-0.30+0.07i$
$(\phi_1 \rightarrow \phi_2 \rightarrow \phi_3)$	$0.02-0.01i$	$0.03-0.05i$
$(\phi_1 \rightarrow \phi_4 \rightarrow \phi_3)$	$0.01+0.02i$	$-0.02i$
$(\phi_1 \rightarrow \phi_2 \rightarrow \phi_1 \rightarrow \phi_3)$	$0.01-0.02i$	0

little dynamical behavior. Figure 8 shows $|R_{11}^{\dagger}(t)|$ and $|R_{31}^{\dagger}(t)|$ for the cases of 5, 8, and 30 iterations. Comparison to Fig. 1 shows that they, respectively, resemble $|U_{11}(t)|$ and $|U_{31}(t)|$ more as the number of iterations increase, indicating that $R^{\dagger}(t)$ is capturing more of the system dynamics.

System C was also subjected to the two point optimization procedure detailed in Sec. III C. The procedure needs to be applied a number of times in order to significantly reduce the Hamiltonian norm as defined in Eq. (14). Figure 9 shows the Hamiltonian norm J as a function of the number of iterations of the procedure. The two point optimization cannot drive the dynamics of $H_R(t)$ to zero [i.e., to lie fully in the representation transformation $R(t)$], because the new basis and the old basis are forced to coincide at the times $t=0$ and $t=T$. Therefore, $U(T)=W_R(T)$, and consequently population transfer in the old and new representations must be the same. As a result, the Hamiltonian norm converges to some nonzero value as the number of iterations increases. It was found that the mechanistic complexity for $W_R(T)$ was not significantly reduced. This means that the transformation was effective in reducing the Hamiltonian norm, but less effective in reducing dynamical complexity.

In order to understand how the latter behavior is tied to features of the system dynamics, a new system D was created for the two point algorithm, retaining the control field and H_0 from system C, but with a new dipole matrix μ. The nonzero elements of μ are $\mu_{12}=1.653$, $\mu_{13}=1.054$, $\mu_{14}=1.6$, $\mu_{23}=0.914$, and $\mu_{34}=0.79$ ($\mu_{ij}=\mu_{ji}$). Figure 10 shows the amplitudes of different mechanistic orders of $U_{31}(T)$ in the original representation, and of $W_{\phi_3,\phi_1}(T)$ for the transformations corresponding to 5 and 30 iterations. The case of $U_{31}(T)$ for system D in Fig. 10 should be compared to that of system C in Fig. 7, where it is evident that system D has a more elaborate, higher order mechanism. The population transfer $|1\rangle \rightarrow |3\rangle$ in the representation of the eigenstates of H_0 yields significant contributions up to ninth order. On the other hand, in the optimized representation after 30 iterations, the same transfer $|\phi_1\rangle \rightarrow |\phi_3\rangle$ involves only up to fifth order terms. Figure 11 shows $|\phi_1\rangle = R^{\dagger}(t)|1\rangle$ for the case of 30 iterations. As the transformation is constrained to return to the identity at $t=T$, the transformed and original basis are the same at the beginning and end points. Some illustrative pathways of the mechanism in the original representation and for 30 iterations are listed in Table IV. The mechanism in the new representation is significantly simpler than that in the original one. Once again, there is a choice to be made in the number of iterations, representing the trade off between representation complexity and Hamiltonian dynamical com-
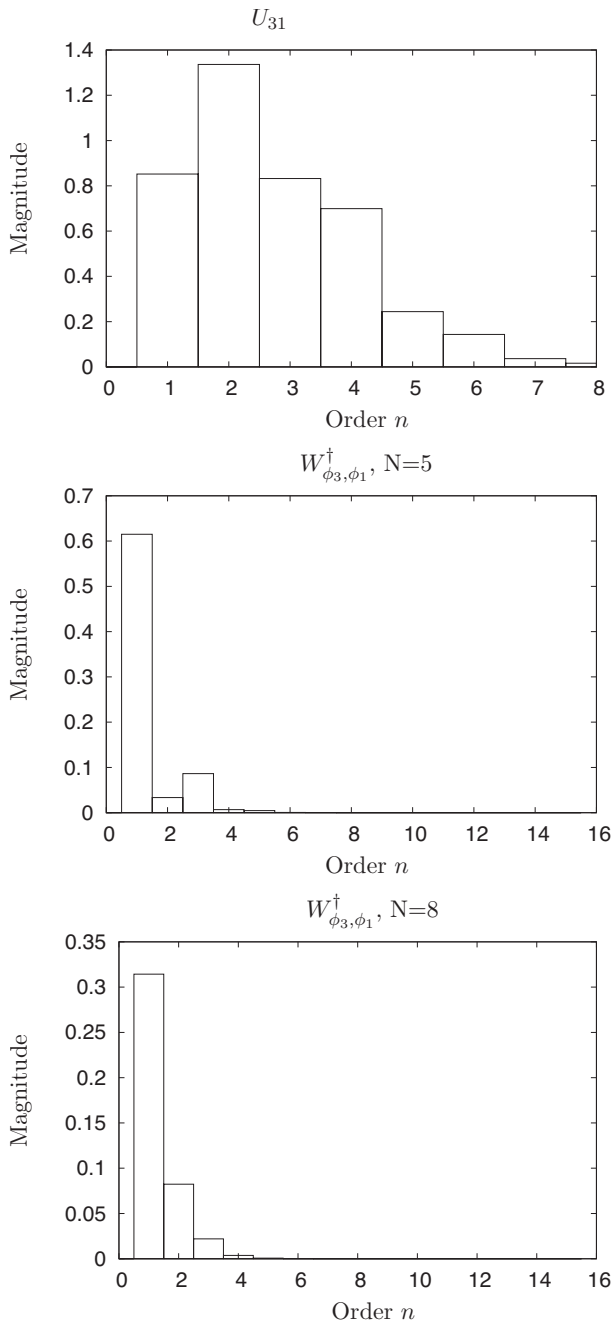
FIG. 7. This figure compares the contributions of different orders of interaction for system C in the original representation $[U_{31}(T)]$ to those of W_{ϕ_3,ϕ_1} for $N=5$ and $N=8$, following the procedure in Sec. IV B. As for the case of Fig. 5, the magnitudes of higher order interactions diminish as N is increased, indicating that the mechanism contained in W gets simpler.

plexity. The reason that system D showed a significant simplification of its mechanism as compared to system C appears to arise from the dynamics induced in system D being more complex, thereby permitting more opportunities for mechanism reduction by iterative representation changes.

VI. CONCLUSION

The dynamical mechanism of controlled quantum mechanical system can depend on the choice of representation
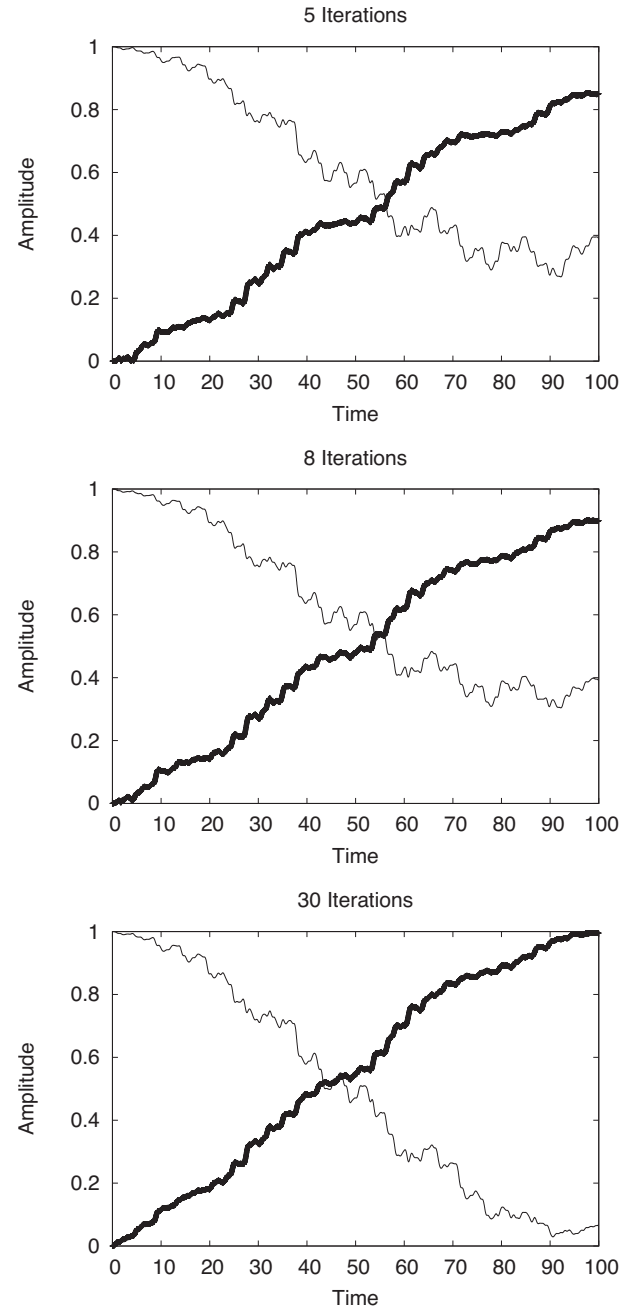
FIG. 8. $|R^{\dagger}_{11}(t)|$ and $|R^{\dagger}_{31}(t)|$ for system C when the Hamiltonian has been iteratively transformed 5, 8, and 30 times. Comparison to Fig. 1 shows how the transformation increasingly captures the dynamics of the original Hamiltonian.

of the system. Although observable expectation values are invariant to the representation, the formulation and understanding of the mechanism, particularly in terms of the amplitudes of significantly contributing quantum pathways, is dependent on the choice of basis states in which the dynamics are followed. The analysis of controlled quantum dynamics first entails a choice of representation and an expression of the Hamiltonian in that representation, followed by an identification of the significantly contributing quantum pathways. An appropriate choice of representation can yield a simpler dynamical picture for the time evolution. In this
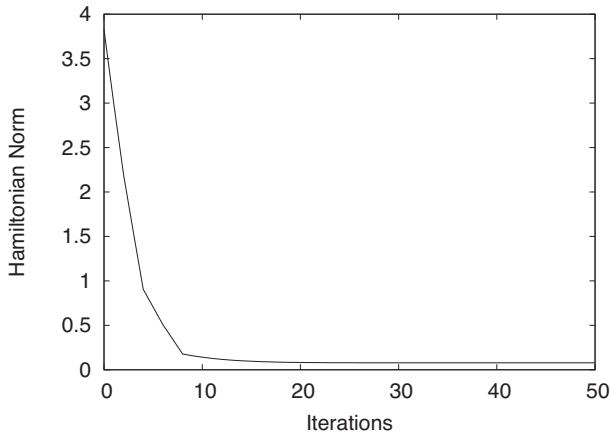
FIG. 9. Hamiltonian norm J of system C as a function of the number of iterations in the two-point, iterative optimal representation procedure outlined in Sec. IV B. For $N > 20$ the norm converges to approximately 0.07.

FIG. 11. $R^{\dagger}(t)|1\rangle = |\phi_1\rangle$ for the two point algorithm. Since the transformation is constrained to be identity at $t = T$, $|\phi_1(0)\rangle = |\phi_1(T)\rangle = |1\rangle$.

work, the criterion of simplicity was quantified in terms of the order of terms contributing to the dynamics within the Dyson expansion. Traditional choices of representation include the eigenstates of the field free Hamiltonian H_0 or the dressed states of the system coupled to the control field. In this work the selection of the representation was set up as an optimization problem. The goal of the optimization is to find a balance between choosing a simple representation for the system and minimizing the dynamical complexity. The structure of the proposed optimization functional was guided by

the criterion of achieving a minimal norm for the Hamiltonian, but other criteria could perhaps be used as well.

This paper started with a general variational formulation in Eq. (13) seeking the representation transformation $R(t)$. The actual operational procedure calls for making a variational *Ansatz*, and as an illustration, all of the techniques in this paper were built around the form in Eq. (28). The ultimate guide is to seek an *Ansatz* that is effective in reducing the norm of $H_R(t)$ while producing an easy means to determine $R(t)$ and ideally admitting a ready physical interpreta-
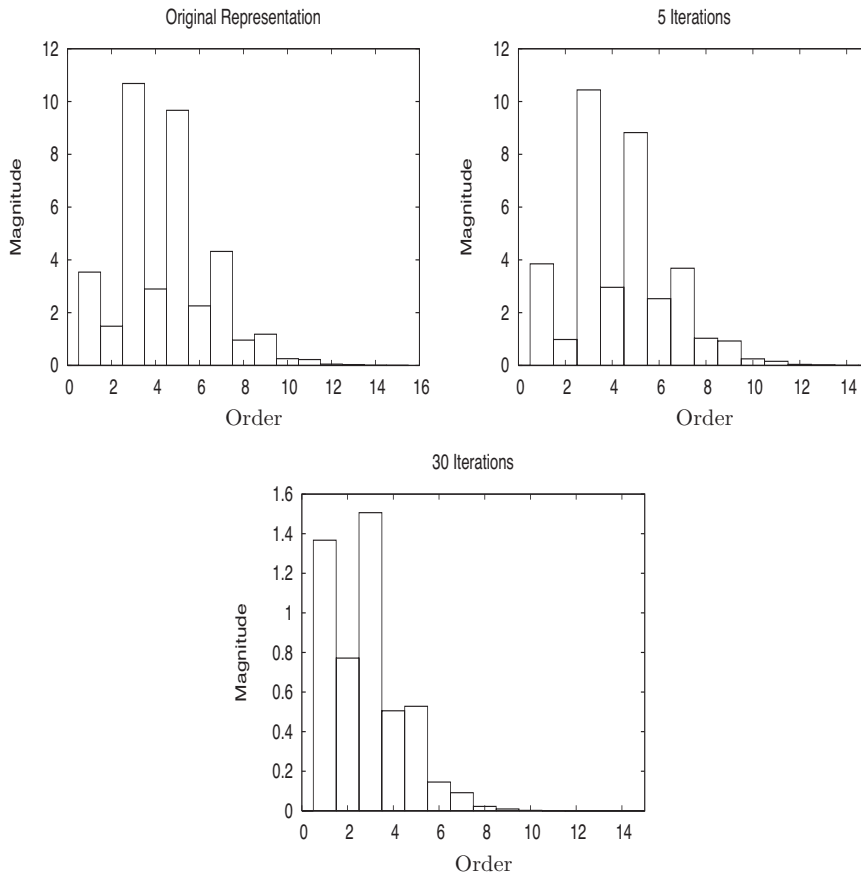
FIG. 10. Mechanistic complexity in U_{31} for system D at different numbers of iterations using the two-point iterative optimal representation procedure of Sec. III C. The procedure transforms the Hamiltonian to a representation where the contribution of higher order terms is reduced as more of the dynamics is contained in the representation. However, since in this case $W_{\phi_3,\phi_1}(T) = U_{31}(T)$, the basis cannot be rotated to be identical to the evolved state in order to capture all the dynamics.

TABLE IV. Mechanism analysis after the two-point iterative optimal representation procedure applied with $n=30$ iterations for system D. Some of the contributing pathways for W_{ϕ_3,ϕ_1} $(T;n=30)$ are listed. For comparison, the amplitudes of the corresponding pathways in the original, unoptimized representation (eigenstates of H_0) are also shown. Although they follow the same transition $|1\rangle \rightarrow |3\rangle$ over the time interval $[0,T]$, the corresponding amplitudes in the original representation are much higher.

Pathway	W_{ϕ_3,ϕ_1} $(T;n=30)$	Pathway	$U_{31}(T)$
$(\phi_1 \rightarrow \phi_3)$	$0.91-0.66i$	$(1 \rightarrow 3)$	$-3.37+1.03i$
$(\phi_1 \rightarrow \phi_2 \rightarrow \phi_3)$	$-0.03-0.02i$	$(1 \rightarrow 2 \rightarrow 3)$	$1.03-0.60i$
$(\phi_1 \rightarrow \phi_4 \rightarrow \phi_3)$	0	$(1 \rightarrow 4 \rightarrow 3)$	$0.26-0.13i$
$(\phi_1 \rightarrow \phi_3 \rightarrow \phi_1 \rightarrow \phi_3)$	$-0.31+0.30i$	$(1 \rightarrow 3 \rightarrow 1 \rightarrow 3)$	$7.03-2.19i$

tion for $R(t)$. The challenge is clear and the variational formulation provides a solid basis for testing various choices.

A procedure was set up to solve the optimization problem. As a simple test, this formalism was shown to be effective in capturing the dynamics of systems obeying the RWA. The method was generalized in order to treat the dynamics of more complex systems. Two procedures were developed which generated a sequence of representation changes of increasing complexity, which captured more of the system dynamics in the representation itself, and yielded increasingly simpler mechanisms. The procedures allowed for choosing an appropriate balance between the representation and the dynamical complexity. Additionally, an extension of these procedures was introduced to fix the representation at initial and final times, taking into account typical constraints in optimal control experiments, where the final state may be of paramount interest, carrying with it a particularly desired representation.

As the different examples of this paper show, the choice of representation for HE can give alternative perspectives to the meaning of control mechanism. Previous work on mechanism analysis helped to generate an understanding of the dynamics by grouping pathways into classes, such as composite pathways [13]. In a complementary fashion, this work shows that the system may be rotated into a representation where the dynamics are simple enough to be captured in a few pathways. Finally, the ability to find representations of reduced dynamical control complexity suggests that simplified models may exist to describe controlled dynamics. The development of the latter topic is also linked to finding representations that are amenable to "simple understanding." The flexibility of the variational formulation opens up a means to determining such models.

[1] S. Shi and H. Rabitz, J. Chem. Phys. **92**, 364 (1989).

[2] R. S. Judson and H. Rabitz, Phys. Rev. Lett. **68**, 1500 (1992).

[3] W. S. Warren, H. Rabitz, and M. Dahleh, Science **259**, 1581 (1993).

[4] Y. Maday and G. Turinici, J. Chem. Phys. **118**, 8191 (2003).

[5] A. Assion, T. Baumert, M. Bergt, T. Brixner, B. Kiefer, V. Seyfried, M. Strehle, and G. Gerber, Science **282**, 919 (1998).

[6] D. Meshulach and Y. Silberberg, Nature (London) **396**, 239 (1998).

[7] T. C. Weinacht, J. Ahn, and P. H. Bucksbaum, Nature (London) **397**, 233 (1999).

[8] R. Bartels, S. Backus, E. Zeek, L. Misoguti, G. Vdovin, I. P. Christov, M. M. Murnane, and H. Kapteyn, Nature (London) **406**, 164 (2000).

[9] T. Hornung, R. Meier, and M. Motzkus, Chem. Phys. Lett. **326**, 445 (2000).

[10] R. J. Levis, G. M. Menkir, and H. Rabitz, Science **292**, 709 (2001).

[11] T. Feuer, A. Glass, T. Rozgonyi, R. Sauerberg, and G. Szabo, Chem. Phys. **267**, 223 (2001).

[12] S. Vajda, A. Bartlet, E. C. Kaposta, T. Leisner, C. Lupulescu, S. Minemoto, P. Rosendo-Francisco, and L. Wöste, Chem. Phys. **267**, 231 (2001).

[13] A. Mitra and H. Rabitz, Phys. Rev. A **67**, 033407 (2003).

[14] A. Mitra, I. Sola, and H. Rabitz, Phys. Rev. A **67**, 043409 (2003).

[15] A. Mitra and H. Rabitz, J. Phys. Chem. A **108**, 4778 (2004).

[16] R. W. Sharp and H. Rabitz, J. Chem. Phys. **121**, 4516 (2004).

[17] K. Bergmann, H. Theuer, and B. W. Shore, Rev. Mod. Phys. **70**, 1003 (1998).

[18] B. W. Shore, *The Theory of Coherent Atomic Excitation* (Wiley, New York, 1990).